Polyelectrolyte Brushes: Debye Approximation and Mean-Field Theory

ARTICLE *in* MACROMOLECULES · MARCH 2011

Impact Factor: 5.8 · DOI: 10.1021/ma1024413

5 AUTHORS, INCLUDING:

Jens-Uwe Sommer

Leibniz Institute of Polymer Research Dresden

196 PUBLICATIONS **3,119** CITATIONS

Macromolecules

ARTICLE

pubs.acs.org/Macromolecules

Polyelectrolyte Brushes: Debye Approximation and Mean-Field Theory

Long Chen,[†] Holger Merlitz,[*,†,‡] Su-zhen He,[†,§] Chen-Xu Wu,[*,†] and Jens-Uwe Sommer[‡]

[†]Department of Physics and ITPA, Xiamen University, Xiamen 361005, P. R. China

[‡]Leibniz-Institut für Polymerforschung Dresden, 01069 Dresden, Germany

[§]Department of Electronic Engineering, Putian University, Putian 351100, P. R. China

ABSTRACT: Off-lattice computer simulations of polyelectrolyte brushes are carried out using the Debye approximation with explicit counterions but implicit salt. The results are compared with explicit salt ion simulations and self-consistent field theory. We demonstrate that the data generated with these different techniques are in excellent agreement, thereby confirming the validity of the Debye approximation in the context of polyelectrolyte brushes. The efficiency of the Debye approximation is verified through benchmark computations. Further on, we develop an improved Flory-type mean-field model, based on the original argument by Pincus, but taking into account both the excluded volume and finite extensibility of chains. On the basis of this model, we demonstrate how the interplay of counterion pressure and excluded volume repulsion explains the observed effect of salt on the swelling of the brush under good solvent conditions. The brush height as a function of grafting density is investigated, and it is argued that the resulting power law scaling of −1/3 is incapable of distinguishing between excluded volume and electrostatic effects.

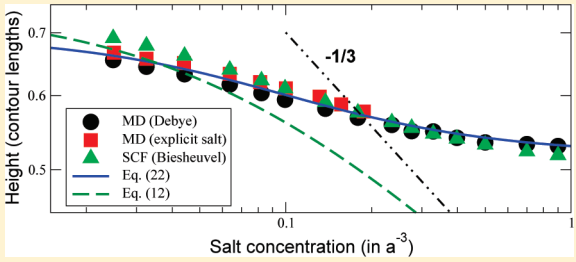

I. INTRODUCTION

Polyelectrolyte brushes consist of charged macromolecules that are end-grafted to a solid interface. They are of importance in various technical applications such as surface modification, colloidal stabilization and lubrication, and abundant in biological systems. Therefore, polyelectrolyte brushes have received a considerable interest in theoretical studies[1−5] as well as in experiments[6−9] during the past two decades. Recent computational studies have further deepened our understanding of the complex interactions of polyelectrolyte brushes and mobile ions.[10−14] As a matter of fact, the simulation of salted polymer brushes remains a challenging task because of the long-range character of the interaction and the large number of mobile salt ions to be accounted for.

The properties of polyelectrolyte brushes have been approximated by Pincus using a Flory-type approach,[1] demonstrating that the salt concentration is among the vital parameters which define the physical properties of the brush. There exist a number of studies in which the influence of varying salt concentration on a charged brush has been addressed.[12−14] At the same time, self-consistent field (SCF) theory has been applied in order to approximate some of the most prominent structural features of charged brushes,[4,15,16] and recently, a novel off-lattice SCF theory has been presented by Biesheuvel et al.,[5] the validity of which has been verified by the authors through molecular dynamics (MD) simulations.[14]

The question arises whether or not the significant computational investment required for the MD simulations with explicit salt could be reduced through the introduction of the Debye approximation, featuring an implicit salt model. The evaluation of this question was among the primary tasks of the present work. A series of studies[17,18] in which the electrostatic interaction was implemented in terms of the Debye approximation have been presented in the past. Among others, Micka et al.[19] have analyzed the dependence of the persistence length of weakly charged polyelectrolytes on the Debye screening length, and Stevens et al.[20] studied observables like osmotic pressure, end-to-end distance, and the structure factor of polyelectrolyte solutions, whereas Schäfer et al.[21] investigated features of the single chain structure factor through Monte Carlo simulations.

Our work is organized as follows. In section II the simulation model is described, followed by the definition of the relevant simulation parameters in section III. After determination of the cutoff of the Debye potential in section IV, the vertical charge distributions of the brushes and mobile ions are analyzed in section V. Here we will demonstrate how the Debye approximation is capable of generating the correct amount of osmotic ion pressure despite of its apparent failure to satisfy local electroneutrality. In section VI we shortly discuss the SCF approach used for this work, and in section VII a short summary of Pincus' mean-field approach is presented, including the generalized formula that does not rely on the strong screening limit. Our simulations indicate a failure of Pincus' approach to represent polymer brushes in good solvent within the range of parameters

Received: October 26, 2010
Revised: January 28, 2011
Published: March 15, 2011

we have studied. In section VIII we therefore develop an extended Flory-type approach that properly accounts for excluded volume effects and that exhibits an excellent agreement with the simulations. The computational efficiency of the Debye approximation, in comparison with the explicit salt simulations, is discussed in the Appendix.

II. SIMULATION MODEL AND METHOD

The polyelectrolyte brush was modeled as $M = 64$ freely jointed bead spring chains, anchored at one end to an uncharged planar surface to form a regular 8×8 square grid. The chains were monodisperse and modeled as N spherical beads. The rectangular simulation box with the dimension of $L \times L \times L_z$ had periodic boundaries in both (horizontal) $x-y$ directions, while the (vertical) height was restricted by a wall to confine the salt ions inside the system. According to previous studies, a vertical box dimension of twice the chain contour length is sufficient to deliver reliable results for the brush properties;[13] hence, this was the choice of our box height. The grafting density of the brush is defined as $\sigma = M/L^2$. To achieve electroneutrality of the system, $M \times N \times f$ counterions were added to the simulation box, where $f = 1$ stands for the charge fraction of the brush (i.e., the fraction of charged monomers; we consider only monovalent charges for both monomers and ions throughout this work). The LAMMPS molecular dynamics package[22] was used to carry out the simulations, the integrator being a Langevin thermostat with implicit solvent. The total interaction potential was composed of four contributions:

$$U_{\mathrm{tot}} = U_{\mathrm{FENE}} + U_{\mathrm{LJ}} + U_{\mathrm{WALL}} + U_{\mathrm{Debye}} \tag{1}$$

The chains were assumed to be in athermal solvent, modeled by a purely repulsive short-range Lennard-Jones potential between beads

$$U_{\mathrm{LJ}}(r) = 4\varepsilon\left[\left(\frac{a}{r}\right)^{12} - \left(\frac{a}{r}\right)^{6} - \left(\frac{a}{r_c}\right)^{12} + \left(\frac{a}{r_c}\right)^{6}\right] \tag{2}$$

where a stands for the bead diameter and ε defines the strength of the interaction. The parameter r_c is the cutoff distance: It is easily verified that without any cutoff ($r_c \to \infty$) this potential has a minimum at $r_{\mathrm{min}} = 2^{1/6}a$ with the depth $U_{\mathrm{LJ}}(r_{\mathrm{min}}) = -\varepsilon$. In turn, once a cutoff $r_c = r_{\mathrm{min}}$ is implemented, and the potential shifted up by ε, all attractive contributions to this potential are eliminated and particles inside an athermal solvent are simulated. Counterions and salt ions as well had a short-range repulsive potential, but of just half of the monomer's interaction length in order to keep their excluded volume effects on a moderate level. This is reasonable for both physical (ions are usually much smaller than statistical monomers) and technical reasons (the SCF theory as well as the mean field theories are entirely neglecting the ion volume).

Beads along the polymer chain were coupled by a FENE (finitely extensible nonlinear elastic) bond potential,[23] with an average bond length $l_b = 0.98a$, close to the bead size a. We are therefore going to use bead size and bond length synonymously in this paper and regard them as a unit length whenever convenient. Two walls (with repulsive LJ potential) were installed to prohibit the mobile ions from leaving the simulation box, one located at the substrate and another one at the upper edge of the simulation box, at a distance of two chain-contour lengths from the substrate.

The Debye approximation employs an exponentially damped Coulomb potential that accounts for the screening by the salt background:

$$U_{\mathrm{Debye}}(r) = k_{\mathrm{B}}T q_i q_j \frac{\lambda_{\mathrm{B}}}{r} \mathrm{e}^{-r/\lambda_{\mathrm{D}}} \tag{3}$$

where q_i and q_j are the charges in units of the elementary charge e and

$$\lambda_{\mathrm{B}} = \frac{e^2}{\varepsilon k_{\mathrm{B}}T} \tag{4}$$

is the Bjerrum length, the distance at which the Coulomb interaction of two unit charges is comparable in magnitude to their thermal energy. The Debye screening length is defined as

$$\lambda_{\mathrm{D}} = \frac{1}{\sqrt{8\pi\lambda_{\mathrm{B}}C_{\mathrm{s}}}} \tag{5}$$

with the background salt concentration C_s, which is defined as the concentration of salt molecules, i.e., pairs of (monovalent) salt ions and counterions.

For comparison, some systems were simulated using explicit salt ions (modeled in the same way as the counterions) and a full long-range Coulomb potential. Details about these explicit salt simulations can be found in ref 14.

III. SYSTEM SETUP

The brushes were initiated as an array of $M = 8 \times 8$ stretched chains made of $N = 32$ beads and grafted in a square lattice pattern onto the substrate. The chains were fully charged (one positive charge on each monomer), and the counterions were monovalent, which implies one counterion for each of the $N \times M$ monomers. The time step was $0.0015\tau_{\mathrm{LJ}}$, where $\tau_{\mathrm{LJ}} = (ma^2/\varepsilon)^{1/2}$ is the Lennard-Jones time and $m = 1$ the monomer mass. The damping constant was equal to one inverse τ_{LJ}.

For relaxation, 4×10^6 simulation steps, corresponding to 6000 LJ times, were carried out. In this way, the system was given sufficient time to reach its statistical equilibrium. During the following several 10^6 simulation steps of data production, the conformations were stored at a frequency of $1/(3\tau_{\mathrm{LJ}})$. The simulations were carried out with a Bjerrum length $\lambda_{\mathrm{B}}/a = 0.1$, at which the brush (in the absence of salt) has entered its osmotic regime even at the lowest grafting density of $\sigma a^2 = 0.05$ that is considered in our simulations (see ref 14 for a detailed discussion of the observable brush regimes).

IV. DEBYE POTENTIAL CUTOFF

The Debye potential has an exponentially damped tail and should be cut in order to save computational resources. The ideal choice for the cutoff distance has to be determined to achieve the right balance between simulation time and residual artifacts that come along with the cutoff.

A couple of test simulations have been carried out, in which the cutoff distance (measured in units of the Debye length) was varied between two and eight. Figure 1 displays the resulting density distributions of the brushes at grafting density $\sigma a^2 = 0.1$. The Bjerrum length was $\lambda_{\mathrm{B}} = 0.1a$ and the Debye length $\lambda_{\mathrm{D}} = a$. The density profiles display just minor differences. The center of mass height of each brush was determined and is shown in the inset of Figure 1: With increasing cutoff length, the brush height is systematically increasing from 0.210 to 0.218 (in units of the

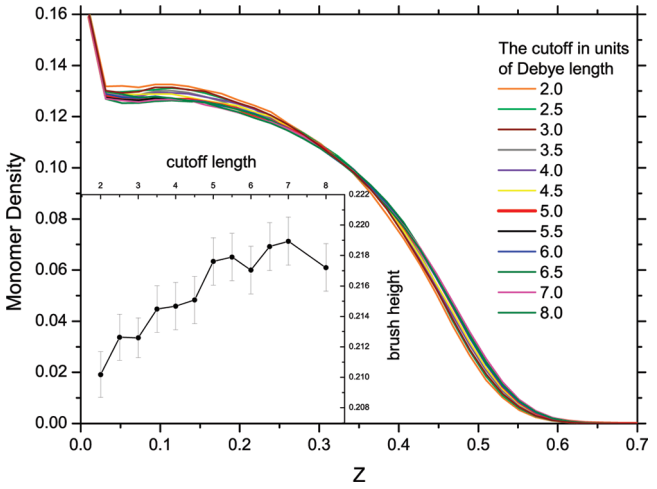

Figure 1. Vertical density profiles of brushes at different cutoff lengths of the Debye potential. The vertical coordinate Z is given in units of the contour length of the chains. Inset: center-of-mass height (units of contour length) of the brush as a function of the cutoff length (units of the Debye length).

chain contour length), i.e., by roughly 4%, and then reaching a plateau at which the height exhibits fluctuations of the order of half a percent about its average value. This plateau is reached at a cutoff length of five Debye lengths, and throughout the paper we are using this value as our cutoff for the Debye potential. This choice coincides with ref 21 in which isotropic solutions of polyelectrolytes were studied.

V. CHARGE DISTRIBUTIONS

In order to understand the character of the Debye approximation, it is instructive to study the vertical distribution of charges in the simulation box. For these simulations, a moderate grafting density of $\sigma a^2 = 0.1$ was chosen. In the absence of salt, this brush would be in its osmotic regime; i.e., the majority of counterions would remain trapped inside the brush, with the exception of a narrow layer of counterions being localized just above the brush surface. Such a brush satisfies the condition of local electroneutrality quite well; i.e., each cross section of the brush may be regarded as approximately neutral.[3,14] After the addition of monovalent salt ions, the monomer counterions and salt counterions are indistinguishable and able to exchange one another. Additionally, salt co-ions are capable of entering the brush regime and hence modifying the number of mobile ions inside the brush.

Figure 2 shows a snapshot of a typical system setup, including counterions and explicit salt ions, after relaxation. When averaged over a large number of conformations, charge distributions, as displayed in Figure 3, can be obtained. This figure displays vertical charge distributions in the case of low salt background concentration $C_s a^3 = 0.025$. Here we compare the distributions obtained from explicit salt simulations (circles) with the distributions of the Debye (implicit salt) approximation. In the former case, the net charge distribution (solid dots) remains approximately flat and stays close to zero throughout the box—this is the local electroneutrality. A deviation from local electroneutrality occurs near the brush surface (at $Z \approx 0.55$) where a characteristic thin layer of counterions is formed.[3] Above this charged layer, the net charge quickly drops to zero. The situation is different in case of the Debye approximation, where the net charge is the sum of monomers and counterions (solid squares). This quantity is positive inside the brush and negative outside, and it does not drop to zero above the brush surface. This implies that counterions are capable of leaving the brush body and moving freely within the boundaries of the system (only limited by the wall at $Z = 2$ contour lengths). Hence, the Debye approximation does not seem to obey the local electroneutrality approximation. In fact, it does so, but implicitly: If we compare the counterions in the Debye approximation with the monomer counterions of the explicit salt simulation (excluding the salt counterions), we observe almost identical density distributions (blank squares vs triangles). With explicit salt, and inside a finite system, some of the primordial counterions are replaced by salt counterions which enter the brush and subsequently set free. Those salt ions are implicitly present in the Debye approximation, and the fact that both (monomer) counterion distributions coincide implies that the screening effects are analogous in both systems. Hence, the Debye approximation does satisfy local electroneutrality, but implicitly, and a naive count of charges in the system (solid squares) does not exhibit the expected annulation of charges.

Not surprisingly, the above-discussed phenomena are even more pronounced at high salt concentrations (data not shown). Here, the monomer counterions are almost uniformly distributed inside the system, and their finite concentration is determined by the size of the simulation box. Once again, their concentrations are the same regardless whether or not the salt is treated explicitly or through the Debye approximation. In this context we shall address the question whether or not explicit counterions are at all required for the Debye approximation. The answer is affirmative as long as the system is of finite size, since in this case the salt counterions are diluting, but not diminishing, the counterion concentration. If the finite brush were put into an infinite box with constant salt background, then the infinite number of salt counterions would dilute the monomer counterions (which are of finite number) to a concentration of zero, and in this case the explicit treatment of counterions would become obsolete.

VI. OFF-LATTICE SCF THEORY

For comparison, the SCF approach by Biesheuvel et al. has been implemented.[5] This approach is based on the local electroneutrality assumption to eliminate the electrostatic potential, so that an explicit solution of the Poisson−Boltzmann equation can be avoided. The resulting equations are therefore rather simple and require very little computational resources. This approach is restricted to the osmotic regime of the brush, since in the weak charge regime the local electroneutrality condition is not satisfied. For a detailed discussion of its implementation and properties we refer to our previous work.[14] The only modification we have implemented in the present work concerns the Kuhn length of the polymers: The SCF potential contains the Kuhn length as a parameter, and as per definition it refers to the neutral Kuhn length of the ideal chain. Our coarse-grained model is not ideal, however, and considering its excluded volume interactions, the bond length does not exactly correspond to one Kuhn length. We have therefore carried out simulations of neutral brushes at different grafting densities and compared their heights with the SCF results. We obtained a good fit of the neutral brush heights when assuming a Kuhn length of $k = 1.12a$, i.e., slightly larger

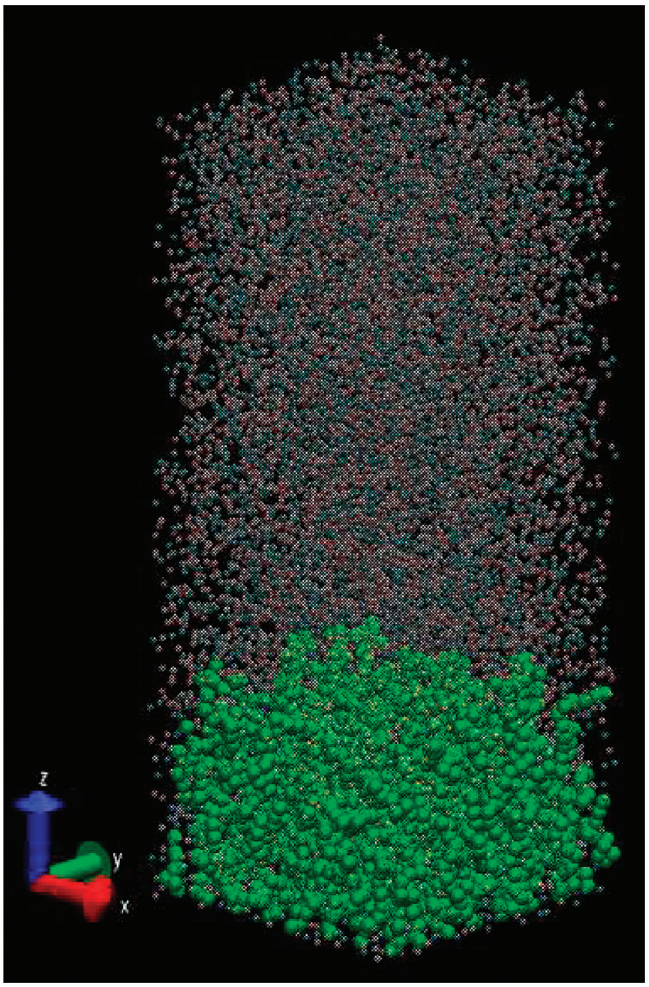

Figure 2. Snapshot of a system with explicit salt ions. The brush was grafted at a density $\sigma = 0.1a^{-2}$ (a being the diameter of each monomer, green) and salt molecule concentration of $C_s = 0.19a^{-3}$. The ions of diameter $a/2$ are plotted transparent to improve visibility of the brush. Monomer counterions are white; salt ions are red and blue.

than the bond length, and we have used that value for our charged brushes throughout this paper.

VII. PINCUS' APPROACH TO THE BRUSH HEIGHT

In his classical paper,[1] Pincus assumed local electroneutrality throughout the brush, which, in the absence of salt, and assuming monovalent ions, implies that the counterion distribution coincides with the monomer distribution. If the brush profile is approximated as a step-function of height H ("box model"), we obtain for the concentration of charged monomers the relation

$$C_q = fC_{\mathrm{mon}} = \frac{fN\sigma}{H} \tag{6}$$

where f denotes the fraction of charged monomers (=1 in our system), C_{mon} the monomer concentration, σ the grafting density, N the number of monomers per chain. For sufficiently diluted ions one may apply van't Hoff's approximation (in units of k_BT)

$$\pi = C_q \tag{7}$$

for the osmotic pressure of the counterions which is identical to the ideal gas law. The presence of added salt was approximated in the original work by the following expression for the osmotic pressure:

$$\pi \sim \frac{{C_q}^2}{C_s + C_q} \tag{8}$$

where C_s is the concentration of the (monovalent) salt background. In order to derive the law for the brush height, Pincus has assumed a balance between the osmotic pressure caused by the ions and the elastic pressure due to chain stretching. This corresponds to a Flory-type approach to the free energy of the brush using a box-shaped monomer profile. By approximating the elastic force through the linear Hooke law (Gaussian chain limit), one arrives at the relation

$$\pi \sim \frac{{C_q}^2}{C_q + C_s} \sim \frac{H\sigma}{Na^2} \tag{9}$$

Considering the concentration C_q itself being inversely proportional to the brush height, eq 6, this leads to a third-order polynomial for the brush height. The strong screening limit is given by $C_s \gg C_q$. Here, the result for the ions' osmotic pressure simplifies to

$$\pi \sim \frac{{C_q}^2}{C_s} \sim \frac{H\sigma}{Na^2} \tag{10}$$

being easily solved to

$$H \sim Na\left(\frac{f^2\sigma}{aC_s}\right)^{1/3} \tag{11}$$

The more general case of moderate salt content, eq 9, leads to the following implicit relation for the brush height

$$H \sim \frac{Na^2}{\sigma}\frac{{C_q}^2}{C_q + C_s} \tag{12}$$

Taking into account eq 6, the resulting polynomial can be solved exactly for H, with a single real-valued root (while two other roots are imaginary and hence nonphysical).

Figure 4 displays the brush heights (in units of the contour length), obtained with different simulation methods and SCF theory, as a function of salt concentration. In these simulations, the grafting density was kept constant at $\sigma = 0.1a^{-2}$. The brush heights were determined with a procedure described in ref 14, during which the density profile is analyzed, and the position at which this profile drops to 10% of its value is defined as the brush height (or chain stretch). The simulations and SCF theory are compared with Pincus' general result of eq 12 (dashed curve, an arbitrary prefactor was used to shift Pincus' results into a convenient vertical position). SCF theory, Debye MD, and explicit salt MD deliver consistent results: The brush heights are reduced with increasing salt concentration, and toward the strong screening limit, they begin to level off. This is quite contrary to the functional behavior of eq 12, which does not at all level off, but asymptotically approaches the $-1/3$ power-law scaling of eq 11. Below we will demonstrate that the previously discussed approximation is lacking an appropriate treatment of the excluded volume effects which become important in good solvent and at higher salt concentrations. We shall introduce an extended Flory-type model in the following section, through

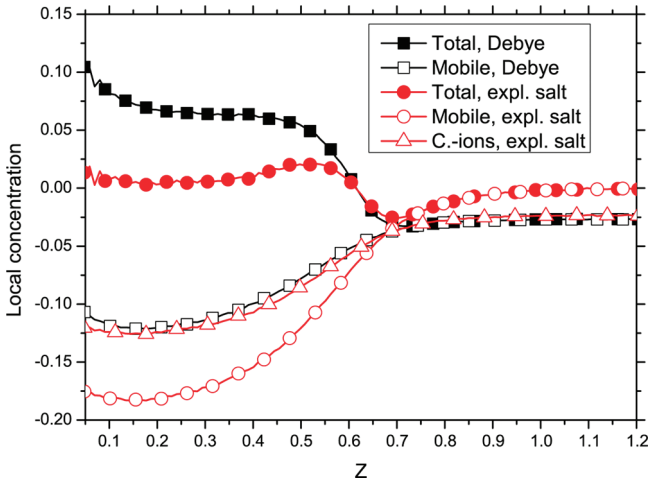

Figure 3. Comparison of the normalized vertical charge distributions of different components of the systems (total charge, solid symbols; mobile ions, blank symbols) with explicit salt (circles) and in the Debye approximation (squares). Triangles stand for monomer counterions that exclusively stem from the brush. Grafting density: $\sigma = 0.1a^{-2}$; salt concentration: $C_s a^3 = 0.025$. Note that the simulation box extends all the way to the coordinate $Z = 2$ (units of chain contour length).

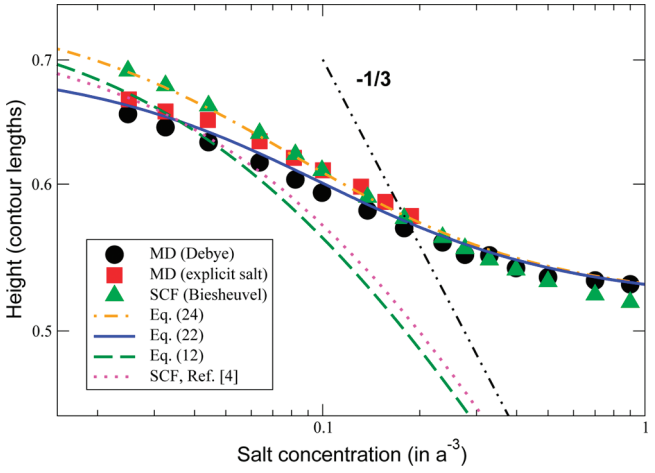

Figure 4. Brush height (in units of contour length) as a function of salt concentration at grafting density $\sigma = 0.1a^{-2}$. Counterion pressure only (Pincus), eq 12, including its strong-screening limit, eq 11, which leads to the $-1/3$ power-law scaling, fail to reproduce the data even on a qualitative level. The introduction of excluded volume repulsion leads to a qualitative agreement, eq 24. The additional condition of finite extensibility delivers a quantitative description of the data, eq 22. The dotted curve corresponds to the SCF approach of Zhulina et al.

which we will achieve a quantitative agreement with the simulation results.

VIII. CONTRIBUTION OF COUNTERION PRESSURE AND EXCLUDED VOLUME TO BRUSH SWELLING

The starting point is an equation that balances three pressures

$$\pi_{cb} + \pi_{el} + \pi_{ev} = 0 \tag{13}$$

according to the osmotic pressure of mobile ions (counterions, salt ions), the negative elastic pressure due to chain stretching and the pressure due to pairwise excluded volume interactions.

The first term in eq 13 can be expressed by charge balance (in units of k_BT) in accordance with the Donnan equilibrium[2]

$$\pi_{cb} = C_q[\sqrt{1+y^2} - y] \tag{14}$$

where $y = 2C_s/C_q$ equals twice the ratio of salt vs charged monomer concentration. In the limit of low salt concentrations, $y \to 0$, van't Hoff's law, eq 7, is obtained. For high salt concentration, $y \gg 1$, one obtains $\pi_{cb} \sim C_q^2/C_s$, which is equivalent to eq 10. We note that the latter result corresponds to an effective second virial coefficient for the charged monomers which, however, drops to zero at high salt concentration. In this regime the second virial coefficient due to excluded volume repulsion dominates and leads to a saturation of the brush hight.

As before, we assume a boxlike brush profile according to the Alexander model and rewrite eq 6

$$C_{mon} = \frac{\sigma N}{H} = \frac{\sigma}{ar} \tag{15}$$

using the stretching ratio $r = H/(aN)$ that is assumed to be identical for all chains in this simple model. We thus obtain

$$y = \frac{2C_s ar}{f\sigma} \tag{16}$$

The second term in eq 13 can be derived from the free energy of a freely jointed chain[24]

$$F_{el} = \frac{1}{a}\int_0^H L^{-1}\left(\frac{x}{Na}\right) dx \tag{17}$$

Here, L^{-1} is the inverse of the Langevin function $L(x) = \coth(x) - 1/x$, accounting for the finite extensibility of the chain. A convenient approximation of L^{-1} that, contrary to the Taylor expansion, is usable throughout the entire range $0 \le x < 1$ and that retains the pole at $x \to 1$ was presented by Cohen:[25]

$$L^{-1}(x) \approx x\frac{3-x^2}{1-x^2} \tag{18}$$

The elastic osmotic pressure is then derived from the free energy of the total number of M chains:

$$\pi_{el} = -M\frac{\partial F_{el}}{\partial V} = -\frac{\sigma r}{a}\frac{3-r^2}{1-r^2} \tag{19}$$

which, in the low-stretching limit, simplifies to the Gaussian approximation

$$\pi_{el} \approx -\frac{3\sigma}{a} r \tag{20}$$

The third term in eq 13 is derived using the mean-field approximation for the excluded volume interactions

$$\pi_{ev} = v_0 C_{mon}^2 = \frac{v_0\sigma^2}{a^2 r^2} \tag{21}$$

with the (second virial) excluded volume parameter v_0. Collecting all results together into the balance eq 13 yields

$$Afr[\sqrt{1+y^2} - y] - r^3\frac{3-r^2}{1-r^2} + \frac{v_0\sigma}{a} = 0 \tag{22}$$

Note that we have introduced another numerical factor A in front of the first term: The Flory mean-field theory neglects any correlations and therefore overestimates the excluded volume

dx.doi.org/10.1021/ma1024413 |Macromolecules 2011, 44, 3109–3116

effects.[26] This has to be compensated for by the factor $A > 1$, serving as a free fit parameter and being adjusted to the data.

Initially, the equation may be solved for the neutral brush ($f = 0$), in which case the first term is eliminated and the excluded volume v_0 is directly evaluated from the neutral stretching ratio r_0 as

$$v_0 = \frac{a{r_0}^3}{\sigma}\frac{3 - {r_0}^2}{1 - {r_0}^2} \tag{23}$$

A simulation of the neutral system at density $\sigma = 0.1a^{-2}$ delivered a brush height of $r_0 = 0.518$ (the average bond length of $a = 0.98$ being close to unity), yielding $v_0 = 5.2\ a^3$. With this result, the factor A was left as the only free parameter, and after fitting it to the data of the Debye simulation, we obtained a value of $A = 1.6$, arriving at a solution which both qualitatively and quantitatively coincides with the simulations (see Figure 4, solid curve).

It is easily verified that finite extensibility is an important ingredient of the model: If the (approximate) inverse Langevin function in eq 19 is replaced with the Gaussian approximation, eq 20, we arrive at the balance equation

$$Afr[\sqrt{1 + y^2} - y] - 3r^3 + \frac{v_0\sigma}{a} = 0 \tag{24}$$

with ${3r_0}^3 = v_0\sigma/a$ in the limit $f \rightarrow 0$. Once the entire procedure of fitting the parameter A is repeated (yielding $A \approx 1.1$), the resulting curve (dash-dotted curve in Figure 4) displays a merely qualitative agreement with the data. At low salt concentrations, with increasing chain stretch, the finite extensibility of the chain has got a significant impact on the brush height. It should be noted that the close agreement with the SCF data (triangles) is coincidental: The SCF procedure is properly accounting for effects of finite extensibility,[5] and the fact that this method delivers a stretching somewhat higher than the simulations is likely to be related with an overestimated osmotic pressure of the counterions at low salt concentrations: While the SCF assumes a perfect match of both the charged monomer and counterion distributions (leading to local electroneutrality), this match is imperfect in the simulations where a certain fraction of counterions moves above the brush surface, so that local electroneutrality is violated (see section V).

Pincus' strong screening limit, $y \gg 1$, is reached by ignoring the third term in eq 22 and using the Gaussian limit for the elastic contribution. Thus, we obtain

$$r = \left(\frac{Af^2\sigma}{12aC_s}\right)^{1/3} \sim \left(\frac{f^2\sigma}{aC_s}\right)^{1/3} \tag{25}$$

which has the same scaling properties as eq 11. One might argue that in the case of low-density brushes the approximation of $v_0 \rightarrow 0$ and hence the power-law scaling of eq 25 might be valid, but our SCF calculations, obtained for a brush of very low grafting density $\sigma = 0.01$, delivered the opposite (data not shown): Even in this case, the excluded volume effect remains strong enough to prevent the existence of any $r \sim {C_s}^{-1/3}$ power-law scaling regime in a good solvent. We have finally compared our results with another approach, presented by Zhulina et al.[4] Their method is more sophisticated than Pincus', since it is not based on the box model but assumes a parabolic SCF, and it additionally solves the Poisson−Boltzmann equation and does not rely on the local electroneutrality assumption. However, their approach neglects excluded volume effects, which is clearly pointed out in their paper, in which they restrict the validity of their method to brushes in Θ-solvent or marginally good solvent. Their resulting brush heights, numerically obtained from eq 18 in ref 4, coincide well with Pincus' model (after proper rescaling), once again indicating that it is the excluded volume effect in the good solvent that is the missing contribution in their models.

Using the strong screening limit in the Gaussian approximation, eq 24, we arrive at

$$\frac{Af^2\sigma}{4aC_s} - 3r^3 + \frac{v_0\sigma}{a} = 0 \tag{26}$$

and hence

$$r = \left[\frac{\sigma}{3a}\left(v_0 + \frac{Af^2}{4C_s}\right)\right]^{1/3} \tag{27}$$

This relation suggests a power-law scaling of the brush height with the grafting density σ. Generally, in the strong screening limit, the ratio $f^2/4C_s$ to v_0 controls the residual counterion contribution to the swelling, so that for $C_s \gg Af^2/4v_0$ the excluded volume repulsion always dominates.

Figure 5 displays the (center of mass) height of the brush, obtained via Debye MD and SCF theory at a salt concentration of $C_s a^3 \approx 0.18$. The data indicate that the scaling of $r \sim \sigma^{1/3}$, as predicted in eq 27 is in fact observable. As mentioned before, the heights obtained with the SCF are somewhat above the simulated heights, possibly because of the local electroneutrality condition that is not perfectly valid in the simulations, except for the regime of very high salt concentrations. We note again that the residual counterion pressure takes a form of the second virial coefficient. Thus, the purely electrostatic model of Pincus does as well predict a behavior of $H \sim \sigma^{1/3}$ in the strong screening limit. On the basis of this behavior alone, however, we cannot discriminate the electrostatic effects from excluded volume repulsion, and the appropriate scaling in Figure 5 cannot be taken to support the purely electrostatic model as has been frequently done in previous work (see e.g. ref 13).

IX. CONCLUSION

The Debye approximation offers an efficient alternative to explicit salt simulations of polyelectrolyte brushes and delivers results that are consistent with SCF theory. We have argued in section V (Figure 3) that polymer brushes, once approximated with the Debye potential, do no longer exhibit local electroneutrality. However, this condition is satisfied implicitly, and hence their counterion distributions coincide with those of the corresponding explicit salt simulations, yielding a correct contribution of the counterion's osmotic pressure.

The classical Flory-type approach based on ion osmotic pressure as the swelling force, as suggested first by Pincus, cannot properly explain the behavior of charged brushes under good solvent conditions. Here, excluded volume effects contribute essentially—even for fully charged chains as they were used in the present set of simulations. As a result, the brush height saturates at high salt concentrations. We have proposed an extended Flory-type model where both the osmotic pressure caused by the ions and the good solvent (excluded volume) effects have been taken into account. Moreover, we have demonstrated that finite extensibility is of relevance even at moderate grafting densities.

Interestingly, the scaling prediction for the stretching ratio, $r \sim \sigma^{1/3}$, in the limit of high salt concentrations is recovered with

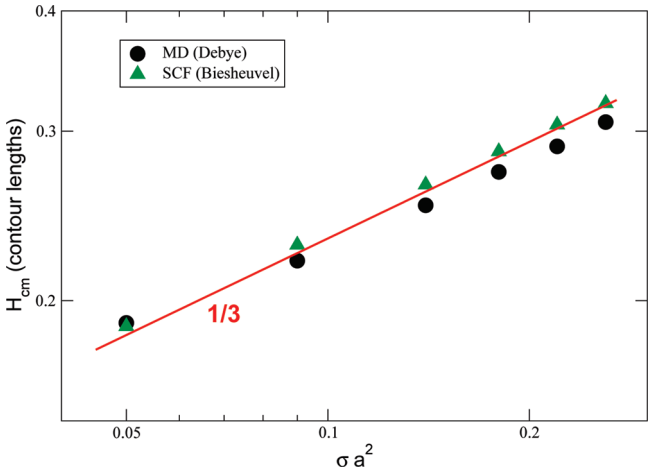

Figure 5. Brush (center of mass) height vs grafting density σ. The height is scaled with the contour length. Salt concentration: $C_s a^3 \approx 0.18$.

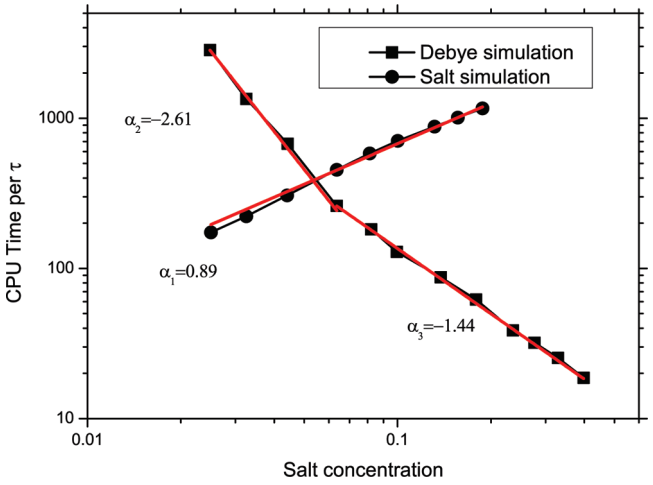

Figure 6. CPU time per τ as a function of the salt concentration.

both the purely electrostatic model and the excluded volume dominated model. This is because in the limit of strong screening the residual osmotic pressure of ions takes the form of the second viral coefficient of the charged monomers in full analogy to the excluded volume effect. The ion effect at high salt concentration, however, is dominant in Θ-solvent or marginally good solvent, where the excluded volume effect is reduced to the third virial coefficient.

To conclude, the methods discussed in the present paper can be applied to other brushlike systems such as polyelectrolyte star polymers or dendrimers, in which case a similar mean-field approach has recently been implemented by one of the authors.[30]

APPENDIX. BENCHMARK SIMULATIONS

When compared to the explicit salt simulations, the Debye approximation necessarily delivers less accurate results due to the neglect of salt ion excluded volume (and other) effects. In order to decide under which conditions this approximation is justified, the computational efficiency has to be taken into account. Figure 6 displays the CPU time required to simulate a period of one Lennard-Jones time for various system setups. The explicit salt simulations (dots) require a CPU time that increases approximately linearly with the salt concentration. This is so because the number of salt ions is increasing linearly, and the LAMMPS simulation software is efficient enough to require just a linear (or, in our case, even slightly sublinear) increase of the pair interaction computations, achieved through neighbor list tables. On the contrary, the Debye approximation requires less CPU time with increasing salt concentration because the cutoff of the interaction potential is dropping along with the Debye screening. There exists a point at which both simulation methods are similarly fast, and for our system this point is reached at a concentration of C_s slightly above $0.05a^{-3}$. Beyond that concentration, the Debye approximation is more efficient than the corresponding explicit salt simulation.

The computational effort of the Debye approximation appears to be growing more rapidly at salt concentrations below $C_s \approx 0.06a^{-3}$. This is a consequence of our particular system setup: Our simulation box was periodic in both lateral dimensions, and to avoid spurious effects, the cutoff of the interaction potential had to be shorter than the dimension of the box. At concentrations $C_s < 0.06a^{-3}$, the Debye length was reaching a size of 1/5 of the box, and since the potential cutoff amounted to five Debye lengths, it was necessary to increase the system size (i.e., the number of chains grafted on the substrate) within that low salt concentration regime. This was not required with the explicit salt simulations because here the pppm method[27−29] properly accounted for the Coulomb interactions of all periodic images.

Finally, the SCF approach that was applied here was by far the most efficient method within its limits of applicability (i.e., the osmotic regime of the brush). The computation of the optimum brush profiles required just a couple of CPU seconds.

AUTHOR INFORMATION

Corresponding Author

*E-mail: merlitz@gmx.de (H.M.); cxwu@xmu.edu.cn (C.-X.W.).

ACKNOWLEDGMENT

This work was partly supported by the National Science Foundation of China under Grants 10225420 and 11074208.

REFERENCES

(1) Pincus, P. *Macromolecules* **1991**, *24*, 2919–2919.
(2) Zhulina, E. B.; Birshtein, T. M. *Macromolecules* **1995**, *28*, 1491–1499.
(3) Borisov, O. V.; Zhulina, E. B.; Birshtein, T. M. *Macromolecules* **1994**, *27*, 4795–4803.
(4) Zhulina, E. B.; Wolterink, J. K.; Borisov, O. V. *Macromolecules* **2000**, *33*, 4945–4953.
(5) Biesheuvel, P. M.; de Vos, W. M.; Amoskov, V. M. *Macromolecules* **2008**, *41*, 6254–6259.
(6) Ahrens, H.; Förster, S.; Helm, C. A. *Phys. Rev. Lett.* **1998**, *81*, 4172–4175.
(7) Mir, Y.; Auroy, P.; Auvray, L. *Phys. Rev. Lett.* **1995**, *75*, 2863–2866.
(8) Romet-Lemonne, G.; Daillant, J.; Guenoun, P.; Yang, J.; Mays, J. W. *Phys. Rev. Lett.* **2004**, *93*, 148301.
(9) Ahrens, H.; Förster, S.; Helm, C. A.; Kumar, N. A.; Naji, A.; Netz, R. R.; Seidel, C. J. *J. Phys. Chem. B* **2004**, *108*, 16870–16876.
(10) Seidel, C. *Macromolecules* **2003**, *36*, 2536–2543.
(11) Csajka, F. S.; Seidel, C. *Macromolecules* **2000**, *33*, 2728–2739.
(12) Rühe, J.; et al. *Adv. Polym. Sci.* **2004**, *165*, 79–150.
(13) Kumar, N. A.; Seidel, C. *Macromolecules* **2005**, *38*, 9341–9350.

(14) He, S.-Z.; Merlitz, H.; Chen, L.; Sommer, J.-U.; Wu, C.-X. *Macromolecules* **2010**, *43*, 7845–7851.
(15) Miklavic, S. J.; Marcelja, S. *J. Phys. Chem.* **1988**, *92*, 6718–6722.
(16) Misra, S.; Varanasi, S. *Macromolecules* **1989**, *22*, 4173–4179.
(17) Chodanowshi, P.; Stoll, S. *J. Chem. Phys.* **2001**, *115*, 4951–4960.
(18) Chodanowshi, P.; Stoll, S. *Macromolecules* **2001**, *34*, 2320–2328.
(19) Micka, U.; Kremer, K. *Phys. Rev. E* **1996**, *54*, 2653–2662.
(20) Stevens, M. J.; Kremer, K. *J. Phys. II* **1996**, *6*, 1607–1613.
(21) Schäfer, H.; Seidel, C. *Macromolecules* **1997**, *30*, 6658–6661.
(22) Plimpton, S. J. *J. Comput. Phys* **1995**, *117*, 1.
(23) Kremer, K. *J. Chem. Phys.* **1990**, *92*, 5057.
(24) Lai, P.-Y.; Halperin, A. *Macromolecules* **1991**, *24*, 4981–4982.
(25) Cohen, A. *Rheol. Acta* **1991**, *30*, 270–273.
(26) deGennes, P.-G. *Scaling Concepts in Polymer Physics*; Cornell University Press: Ithaca, NY, 1979.
(27) Hockney, R.; Eastwood, J. *Computer Simulation Using Particles*; McGraw-Hill: New York, 1981.
(28) Frenkel, D.; Smit, B. *Understanding Molecular Simulations*; Academic Press: San Diego, CA, 2001.
(29) Pollock, E. L.; Glosli, J. *Comput. Phys. Comnun.* **1996**, *95*, 93.
(30) Klos, J. S.; Sommer, J.-U. *Macromolecules* **2010**, *43*, 10659–10667.